HSPG synthesis by zebrafish Ext2 and Extl3 is required for Fgf10 signalling during limb development

William H. J. Norton[1], Johan Ledin[1], Heiner Grandel[2] and Carl J. Neumann[1,*]

[1]European Molecular Biology Laboratory (EMBL), Meyerhofstrasse 1, 69117 Heidelberg, Germany
[2]Max-Planck Institute of Molecular Cell Biology and Genetics, Pfotenhauerstrasse 108, 01307 Dresden, Germany
*Author for correspondence (e-mail: carl.neumann@embl-heidelberg.de)

Accepted 9 September 2005

Development 132, 4963-4973
Published by The Company of Biologists 2005
doi:10.1242/dev.02084

Summary

Heparan sulphate proteoglycans (HSPGs) are known to be crucial for signalling by the secreted Wnt, Hedgehog, Bmp and Fgf proteins during invertebrate development. However, relatively little is known about their effect on developmental signalling in vertebrates. Here, we report the analysis of *daedalus*, a novel zebrafish pectoral fin mutant. Positional cloning identified *fgf10* as the gene disrupted in *daedalus*. We find that *fgf10* mutants strongly resemble zebrafish *ext2* and *extl3* mutants, which encode glycosyltransferases required for heparan sulphate biosynthesis. This suggests that HSPGs are crucial for Fgf10 signalling during limb development. Consistent with this proposal, we observe a strong genetic interaction between *fgf10* and *extl3* mutants. Furthermore, application of Fgf10 protein can rescue target gene activation in *fgf10*, but not in *ext2* or *extl3* mutants. By contrast, application of Fgf4 protein can activate target genes in both *ext2* and *extl3* mutants, indicating that *ext2* and *extl3* are differentially required for Fgf10, but not Fgf4, signalling during limb development. This reveals an unexpected specificity of HSPGs in regulating distinct vertebrate Fgfs.

Key words: Zebrafish, HSPG, Fgf10, Limb development, Ext, Heparan, Heparin

Introduction

The development of metazoan animals is directed by cell-cell signalling mediated by members of the Wnt, Hedgehog (Hh), Bmp and Fgf families of secreted signalling proteins. Recently, extensive biochemical and genetic studies have demonstrated that heparan sulphate proteoglycans (HSPGs) play a crucial role in regulating the extracellular distribution, movement and activity of these signalling factors (reviewed by Esko and Selleck, 2002; Nybakken and Perrimon, 2002; Lin, 2004). HSPGs are a diverse group of macromolecules associated with the cell-surface and extracellular matrix, and consist of a core protein to which heparan sulphate (HS) side chains are attached (reviewed by Esko and Selleck, 2002). HS chains are long unbranched polysaccharides consisting of repeating disaccharide units of uronic acid linked to glucosamine. HS chain synthesis occurs in the Golgi apparatus, and is initiated at the HS attachment sites of core proteins, followed by polymerisation and several modifications (Esko and Selleck, 2002; Nybakken and Perrimon, 2002; Lin, 2004).

The exostosin (ext) gene family has been shown to encode glycosyltransferases that synthesise the polymerisation of HS side chains of HSPGs (reviewed by Zak et al., 2002). Vertebrate exostosin genes include *Ext1* and *Ext2*, as well as the exostosin-like genes *Extl1*, *Extl2*, and *Extl3*. In *Drosophila*, 3 exostosin genes have been identified: *ext1*, *ext2* and *extl3* (Bornemann et al., 2004; Han et al., 2004; Takei et al., 2004). All three *Drosophila* exostosin genes participate in shaping the extracellular morphogen gradients of Hh, Dpp/Bmp and Wg/Wnt, as well as regulating their signalling activity (reviewed by Lin, 2004). Interestingly, the effect of Exostosins on specific signalling proteins is context dependent. For example, although all three *Drosophila* exostosins are crucial for Dpp/Bmp signalling in the wing imaginal disc, they have no effect on Dpp/Bmp signalling during embryogenesis (The et al., 1999; Bornemann et al., 2004; Han et al., 2004; Takei et al., 2004). Likewise, neither Hh, nor Wg/Wnt signalling is defective in *ext2* mutants during embryogenesis (The et al., 1999), indicating that the control of developmental signalling by HSPGs is both signal and context dependent.

Fibroblast growth factors (Fgfs) comprise a large family of signalling molecules involved in regulating many cellular responses during development, and often participate in reciprocal signalling across epithelial-mesenchymal boundaries (reviewed by Ornitz, 2000; Itoh and Ornitz, 2004). A well-studied process in which Fgfs mediate epithelial-mesenchymal interactions is during limb development (reviewed by Johnson and Tabin, 1997; Martin, 1998; Tickle and Munsterberg, 2001). Fgf10 is expressed in the limb bud mesenchyme at very early stages in mouse and chicken embryos, and is required for the activation of genes expressed in the overlying apical ectodermal ridge (AER), including Fgf4 and Fgf8 (Ohuchi et al., 1997; Min et al., 1998; Sekine et al., 1999). Fgf10 binds with highest affinity to the Fgfr2b splice variant of Fgf receptor 2, which is expressed in epithelial cells, whereas Fgf4 and Fgf8 have highest affinity for mesenchymally expressed Fgfr2c (Orr-Urtreger et al., 1993; Ornitz et al., 1996). This scenario suggests a model in which Fgf10 signals to Fgfr2b in the overlying ectoderm, leading to

activation of Fgf4 and Fgf8, which then signal back to the mesenchyme via Fgfr2c to maintain Fgf10 expression. Thus, a positive feedback loop is formed, based on mutual dependence (reviewed by Xu et al., 1999). As in mouse and chick, the zebrafish *fgf10* gene is expressed in the mesenchyme of the pectoral fin buds, which are homologous to tetrapod limb buds (Ng et al., 2002). Following initiation of outgrowth, the limb field becomes patterned along three main axes (Johnson and Tabin, 1997; Martin, 1998; Capdevila and Izpisua Belmonte, 2001). Signals from the AER control limb outgrowth along the proximodistal axis. The anteroposterior axis is patterned by Shh secreted from the zone of polarising activity (ZPA). Finally, the limb bud is patterned along its dorsoventral axis, leading to expression of *Wnt7a* and *Eng1* in dorsal and ventral ectoderm, respectively.

A number of biochemical studies have implicated HS in the regulation of Fgf signalling (reviewed in Ornitz, 2000). Structural studies have led to the proposal that either one HS chain forms a ternary complex with one Fgf and one Fgfr molecule (Schlessinger et al., 2000), or that one HS chain binds to two Fgf molecules to form a dimer bridging two receptors (Pellegrini et al., 2000). Interestingly, as distinct Fgfs differ in the amino acid sequence of their heparin-binding sites, they may have distinct requirements for HS to exert their biological activities (Bellosta et al., 2001). However, in contrast to the wealth of biochemical data, there is a scarcity of in vivo studies addressing the role of HS in Fgf signalling. The first genetic evidence for a role of HSPGs in Fgf signalling came from the observation that *Drosophila* mutants in UDP-glucose dehydrogenase, an enzyme which catalyses the formation of an essential building block of HS polysaccharides, are defective for Fgf signalling (Lin et al., 1999). Recently, a mouse mutant disrupting the same gene was shown to cause gastrulation defects owing to abrogation of Fgf8 signalling (Garcia-Garcia and Anderson, 2003).

Exostosins have so far not been directly linked to Fgf signalling in vivo. Ext1 knockout mice die early, as a result of defective gastrulation (Lin et al., 2000). In these mutants, Indian Hedgehog (Ihh) protein fails to associate with the surface of target cells, suggesting a role for Ext1 in Hh signalling. This proposal is further supported by the observation that Ext1 hypomorphic mutations result in an increase in the range of Ihh signalling during bone development (Koziel et al., 2004). Conditional inactivation of Ext1 in the mouse brain leads to a number of defects, some of which may be caused by a reduction of Fgf8 signalling (Inatani et al., 2003). The zebrafish mutants *dackel* and *boxer* disrupt *ext2* and *extl3* respectively, and these genes are required for axon sorting in the optic tract (Lee et al., 2004). Ext2 and Extl3 are broadly and uniformly expressed during embryogenesis, and disruption of both genes causes a global reduction in HS levels (Lee et al., 2004). Both *dackel* and *boxer* were originally isolated on the basis of their defective pectoral fin development (van Eeden et al., 1996), and *dackel* is known to be required for AER maintenance in the pectoral fin bud (Grandel et al., 2000).

In this study, we investigate how *ext2* and *extl3* mutants affect Fgf signalling during limb development. We show that like *ext2*, *extl3* is required for AER maintenance, although its phenotype is weaker and more variable than that of *ext2*. Both *ext2* and *extl3* show a very similar phenotype to *daedalus*, a novel zebrafish pectoral fin mutant. We find that *daedalus* disrupts *fgf10*, thus suggesting that Fgf10 signalling is affected by Ext2 and Extl3. Consistent with this hypothesis, we find that a partial reduction of *fgf10* levels leads to a strong enhancement of the *extl3* limb phenotype. Furthermore, application of Fgf10 protein rescues target gene expression in *fgf10* mutants, but not in *ext2* or *extl3* mutants, suggesting that activity of these genes is necessary for Fgf10 signalling. Interestingly, application of Fgf4 protein can activate target genes in both *ext2* and *extl3* mutants, thus revealing an unexpected specificity for HSPGs in regulating signalling by distinct vertebrate Fgf ligands.

Materials and methods

Fish stocks

The following alleles were used: *daedalus* (*dae*^{tbvbo}; *dae*^{t24030}); *boxer* (*box*^{tw24}) (van Eeden et al., 1996); and *dackel* (*dak*^{tw25e}) (van Eeden et al., 1996). *dae*$^{-/-}$;*box*$^{-/-}$ double mutants were generated by crossing together *dae*^{tbvbo} and *box*^{tw24}. The *dae*^{tbvbo} and *dae*^{t24030} alleles have very similar phenotypes, but as *dae*^{tbvbo} encodes a null allele, we used these mutants for phenotypic characterisation. In some cases, *dae*^{tbvbo} embryos were genotyped using a SNP. Genomic DNA was amplified with the PCR primers GCTCTTCCCAGTTTTCCGAGCTCCAGGA-CAATGTGCAAATCG (forward) and TCCGTTCTTATCGATCCT-GAG (reverse), followed by digestion with *Taq1*. Wild-type embryos generated a band of 260 bp. *dae*^{tbvbo} mutant embryos were not digested by *Taq1* and produced a band of 300 bp; heterozygous embryos were identified as having two bands (300 bp and 260 bp) following electrophoresis on a 2% agarose gel. The residual 40 bp band formed by digestion of wild-type or heterozygous embryos was run off the gel and is not shown in Fig. 7. Embryos were cultured in E3 medium, with or without the addition of 0.003% 1-Phenyl-2-thiourea (PTU, Sigma) to inhibit pigmentation. Embryos were staged according to hours post fertilisation (hpf) (Westerfield, 1995).

Linkage analysis, genetic mapping, cloning and sequencing

For fine mapping of *dae*, SSLPs were generated by using a zebrafish SSR search website (http://danio.mgh.harvard.edu/markers/ssr.html) in combination with the Sanger genome database. The closest SSLP marker to the *dae* mutation uses the primer pair TCGTCTGTC-AGCTCAACCCTA (forward) and GGTACTAAGTGAAGCACTC-TTACTCT (reverse), at a distance of 0.286 cM (2/698 meioses) upstream of the mutation. The PCR primers CAGACACG-ATCACTACGGACGCTTTAC (forward) and AGCTTGACTAAAT-TCGGATGGTAGGAT (reverse) were designed to amplify a 1061 bp fragment of DNA that included the entire *fgf10* open reading frame. rtPCR was performed using cDNA from both sibling and mutant embryos, followed by cloning of the fragment in the TOPO TA vector (Invitrogen) for sequence analysis.

Microinjection of morpholino oligonucleotides

Fgf10 splice morpholino oligonucleotide (MO) was purchased from GeneTools. The MO, designed to target the exon2-intron2 splice junction, has the sequence GAAAATGATGCTCACCGCCCCGTAG (e2i2 MO). A MO stock solution was formed by dilution in water and was stored at –20°C prior to use. Embryos were injected at the single cell stage with 0.125 mM MO, allowed to develop for 3 days and were then scored for pectoral fin phenotype. Embryos were snap frozen in liquid nitrogen and RNA was subsequently extracted. To confirm splicing defects following MO injection, rtPCR was carried out using the Superscriptase II kit (Invitrogen) and the Fgf10F and Fgf10R primers described above.

Histochemical methods

In situ hybridisation was performed as previously described

(Macdonald et al., 1994). The following mRNA in situ probes were used: *bmp2b* (Martinez-Barbera et al., 1997), *dlx2a* (Akimenko et al., 1994), *dusp6* (Kawakami et al., 2003), *eng1a* (Ekker et al., 1992), *erm1* (Roehl and Nusslein-Volhard, 2001), *fgf4* (Grandel et al., 2000), *fgf8* (Reifers et al., 1998), *fgf10* (Ng et al., 2002), *fgf24* (Fischer et al., 2003), *pea3* (Roehl and Nusslein-Volhard, 2001), *shh* (Krauss et al., 1993), *sp8* (Kawakami et al., 2004), *sp9* (Kawakami et al., 2004), *wnt3l* (Krauss et al., 1992) and *wnt7a* (see below). Alcian Blue staining of cartilage was performed as described previously (Grandel and Schulte-Merker, 1998). Histological sections were obtained by staining cryosections with Methylene Blue (Humphrey and Pittman, 1974).

Cloning of zebrafish *wnt7a*

A novel gene encoding a zebrafish *wnt7a* orthologue was identified as lying between 21837919 and 21842385 bp on chromosome 11 using the zebrafish genome server (http://www.ensembl.org/danio_rerio). rtPCR was performed using the Superscriptase II kit (Invitrogen) and the following primers: GCCGCTGGATTTTTCA-CAT (wnt7aF); TGTGTACACTTCTGTCCGTTCACT (wnt7aR). The amplified fragment was cloned in the TOPO TA vector (Invitrogen) and was sequenced and analysed to confirm its identity (see Fig. S1 in the supplementary material).

Bead implantation

Bead implantation was carried out as described previously (Grandel et al., 2000). Recombinant human Fgf4 and Fgf10 protein (R&D systems) was dissolved at a concentration of 1 μg/μl in phosphate-buffered saline with 0.1% bovine serum albumin. All batches of beads loaded with Fgf10 were tested by implantation into *dae* embryos, and assayed for gene rescue, before using the same batch to implant beads into *dak* or *box* mutant embryos.

Results

Phenotype of *daedalus* mutants

daedalus (*dae*) is a novel zebrafish mutant isolated during a recent large scale genetic screen (Habeck et al., 2002) on the basis of its pectoral fin morphology. At 5 days post fertilisation, mutant larvae have severely truncated pectoral fins (Fig. 1B). They show no other apparent defects, but fail to inflate their swim bladder and most mutants die at 2 weeks of age. In order to examine the fin endoskeleton in *dae* mutants, we performed Alcian Blue staining (Fig. 1C,D) (Grandel and Schulte-Merker, 1998). Wild-type larvae have a pectoral fin skeleton that consists, in proximal-to-distal sequence, of a scapulocoracoid, postcoracoid process and an endoskeletal disk (Fig. 1C). In contrast to this, *dae* mutant embryos lack the entire endoskeletal disk and have a dysmorphic scapulocoracoid with most of the postcoracoid process missing (Fig. 1D). To further characterise the pectoral fin defect in *dae*, we examined transverse sections of 40-hour mutant and sibling embryos stained with Methylene Blue (Fig. 1E,F). Wild-type fin buds have a morphologically distinct apical ridge at this stage, which corresponds to the AER in tetrapods (Fig. 1E) (Grandel and Schulte-Merker, 1998). In contrast to this, mutant fin buds appear smaller and undifferentiated, and do not have an apical ridge, although there is a slight apical thickening (Fig. 1F). These observations indicate that *dae* disrupts a gene required for both the development of distal structures and the integrity of the apical ridge of the zebrafish pectoral fin bud.

Molecular characterisation of *daedalus*

To define the molecular function of *dae*, we identified the gene

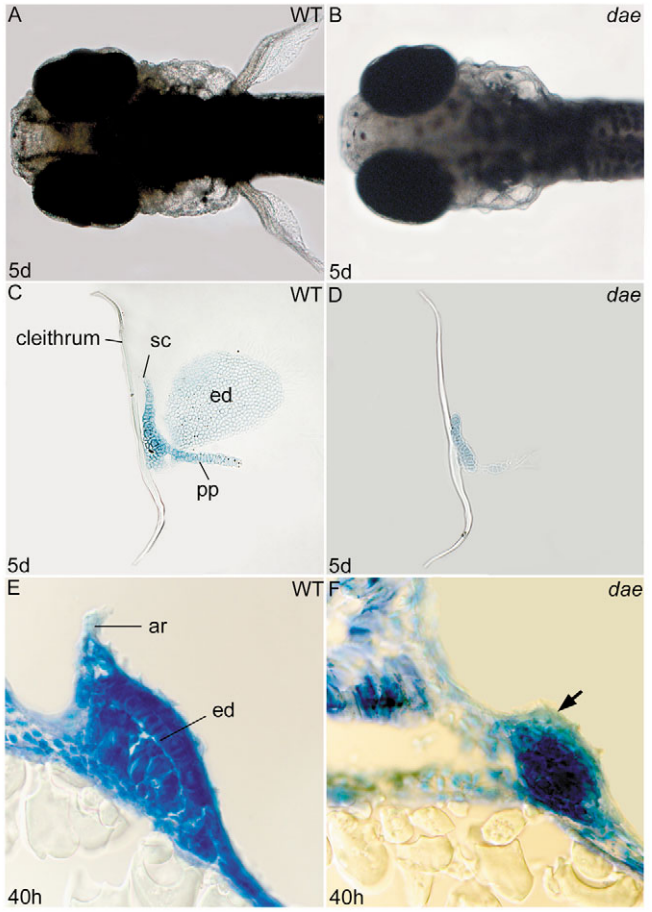

Fig. 1. Phenotype of *daedalus* mutant embryos. (A,B) Dorsal views of live 5-day-old sibling (A) and *dae* mutant (B) larvae, anterior towards the left. *dae* mutants lack pectoral fins, but appear otherwise normal. (C,D) Alcian Blue staining of the pectoral fin endoskeleton. Wild-type endoskeleton (C) consists of a pectoral girdle, postcoracoid process and endoskeletal disk attached to the cleithrum. *dae* mutants (D) retain only a dysmorphic pectoral girdle and cleithrum. (E,F) Transverse cryosections of 40 hpf mutant and sibling embryos stained with Methylene Blue. Mutant embryos (F) have a smaller undifferentiated fin bud, without an apical ridge (ar, arrow), when compared with siblings (E). ed, endoskeletal disc; pp, postcoracoid process; sc, scapulocoracoid.

disrupted by the *dae* mutation (Fig. 2). Initial bulk segregant analysis of pools of 48 sibling and 48 mutant embryos placed the *dae* locus on linkage group 21 (Fig. 2A). Fine mapping using both previously available and novel simple sequence length polymorphisms (SSLPs), placed *dae* within an interval that corresponds to 0.97 cM. Of five genes located between the two closest SSLP markers, *fgf10* was the best candidate for the mutated gene (Fig. 2A). We cloned and sequenced the entire *fgf10* open reading frame of both *dae* alleles. dae^{tbvbo} was found to have a lysine (aaa) to stop (taa) change at amino acid position 5, thus generating a protein null allele. dae^{t24030} encodes an amino acid substitution of methionine (atg) to valine (gtg) at position 170 (Fig. 2B). To further confirm that disruption of *fgf10* causes the *dae* phenotype, we designed a morpholino (MO) to target the exon2-intron2 splice junction of *fgf10* (e2i2 MO; Fig. 2B) and injected this into wild-type

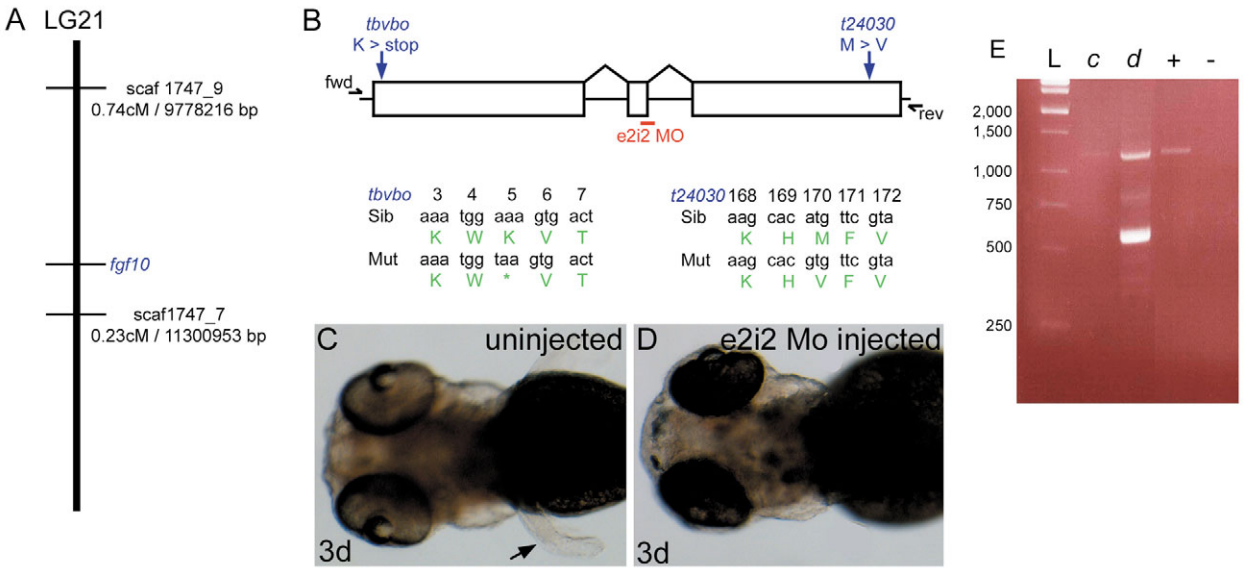

Fig. 2. Positional cloning of the *dae* locus. (A) SSLP analysis places the *dae* mutation between two novel SSLP markers, scaf1747_9 (6/810 meioses) and scaf1747_7 (2/698 meioses) on linkage group 21. The *fgf10* gene was subsequently identified as a candidate for *dae*. (B) The *tbvbo* allele has a K to stop mutation in amino acid 5, and the *t24030* allele has an M to V mutation within amino acid 170 of Fgf10. (C,D) Injection of an Fgf10 morpholino directed against the exon2/intron2 splice acceptor site [e2i2 MO (red bar in B)] into wild-type embryos phenocopies the *dae* mutation. Injection of 0.125 mM morpholino (D) causes a severe truncation of the pectoral fin, identical to the phenotype seen in *dae*. (E) PCR amplification of the *fgf10* open reading frame demonstrates splicing defects following morpholino injection (primer positions indicated in B). L, ladder; –, negative control; +, positive control; *c*, uninjected (compare with C); *d*, MO injected, i.e. *dae*-like phenotype (compare with D).

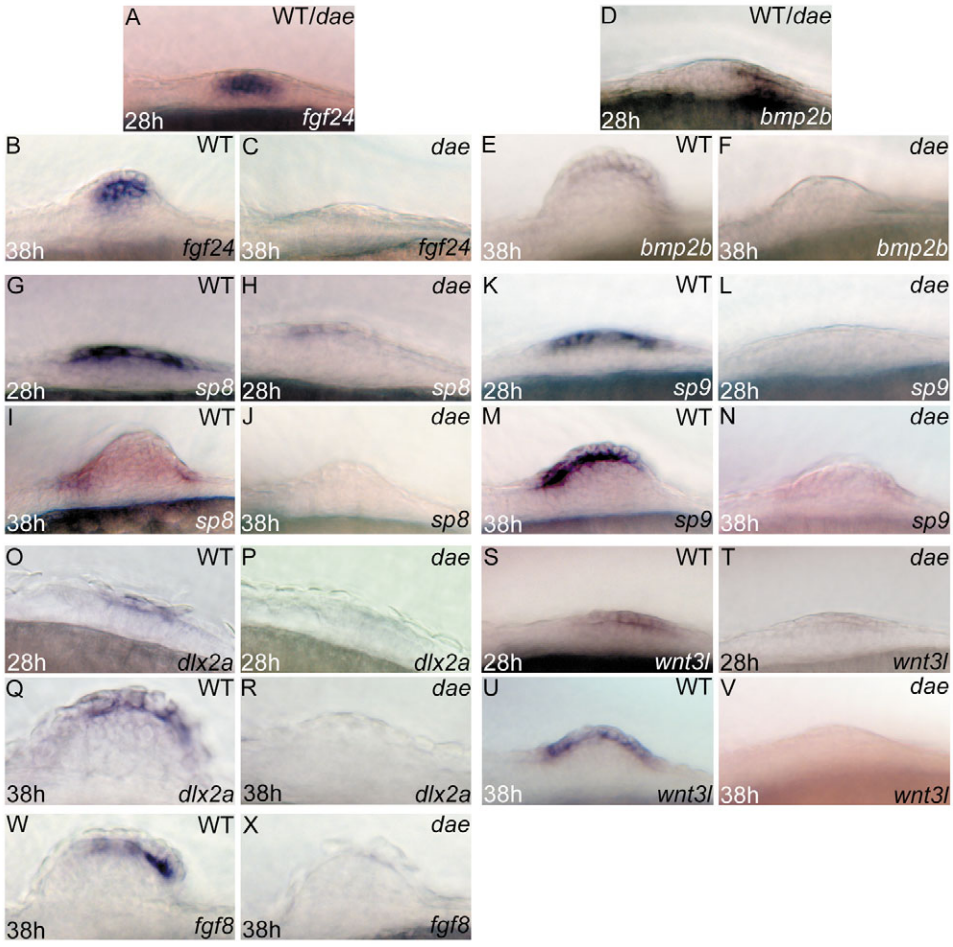

Fig. 3. *fgf10/dae* mutant embryos have reduced expression of AER markers. Lateral views of wild-type (B,E,G,K,I,M,O,S,Q,U,W) and mutant fins (C,F,H,L,J,N,P,T,R,V,X), with anterior towards left. At 28 hpf, expression of *fgf24* and *bmp2b* appears indistinguishable in wild-type and *fgf10/dae* (A,D). Expression of *sp8* is weakly reduced in *dae* (H) but *sp9* (L), *dlx2a* (P) and *wnt3l* (T) expression is strongly reduced in mutants. By 38 hpf, expression of all ridge markers analysed is reduced in *fgf10/dae* (C,F,J,N,R,V,X) when compared with siblings (B,E,I,M,Q,U,W).

embryos at the single cell stage. Injected embryos showed a striking *dae* phenocopy (52% injected embryos; Fig. 2D). We analysed splicing defects following MO injection by extracting RNA from morphant embryos and performing rtPCR. As expected, the morphant rtPCR reaction predominantly generated a smaller band than the full-length transcript found in uninjected siblings (Fig. 2E), confirming that aberrant splicing had occurred (Draper et al., 2001). Taken together, these data indicate that *dae* disrupts the zebrafish *fgf10* gene.

AER development is severely disrupted in *fgf10/dae* mutants

As mouse Fgf10 is required for the establishment of the AER (Min et al., 1998; Sekine et al., 1999), we analysed the expression of AER markers by in situ hybridisation in *fgf10/dae* mutant and sibling embryos. *fgf24* acts upstream of *fgf10* during fin development (Fischer et al., 2003). We therefore examined the early expression of *fgf24* in *dae*. At 28 hpf, expression of *fgf24* in the fin bud is similar in wild-type and *dae* (Fig. 3A). However, by 38 hpf, expression of *fgf24* is absent in *dae* (Fig. 3B,C), suggesting that *fgf10* activity is necessary to maintain *fgf24* expression during development. At early stages of fin development (28 hpf), expression of the ectodermal markers *bmp2b* (Fig. 3D) and *sp8* (Fig. 3H) is present at reduced levels in *fgf10/dae*. However, *sp9*, *dlx2a* and *wnt3l* expression (Krauss et al., 1992; Akimenko et al., 1994; Kawakami et al., 2003) (Fig. 3K,L,O,P,S,T) is strongly reduced even at early stages, indicating that zebrafish Fgf10 already contributes to signalling from the mesenchyme to the ectoderm at this stage. By 38 hpf of development, expression of all AER markers analysed, including *bmp2b* (Fig. 3E,F), *sp8* (Fig. 3I,J), *dlx2a* (Fig. 3Q,R), *fgf8* (Fig. 3W,X), *sp9* (Fig. 3M,N), *wnt3l* (Fig. 3U,V) and *fgf4* (data not shown) is absent from the fin ectoderm in *dae*. Taken together, these results indicate that zebrafish *fgf10/dae* is crucial for AER induction and maintenance. At early stages, there is a low level of *sp8* and *bmp2b* expression in the AER of *fgf10/dae* mutants, while all AER markers are completely lost in *fgf10/dae* mutants at later stages.

Targets of Fgf signalling are down regulated in *fgf10/dae* mutants

We next analysed the expression of several genes known to be targets of Fgf signalling during limb development. *shh*, which is expressed in the zone of polarising activity (ZPA), depends on Fgf4 and Fgf8 signalling from the AER (Sun et al., 2002). At 28 hpf, we detected normal expression of *shh* in *fgf10/dae* fin buds (Fig. 4A,B), but we observed a strong reduction of *shh* expression by 38 hpf (Fig. 4C,D). Similarly, the expression of direct Fgf target genes such as *pea3*, *erm1* (Roehl and Nusslein-Volhard, 2001) and *dusp6* (formerly *mkp3*) (Kawakami et al., 2003) was present at 28 hpf, but absent by 38 hpf of development (Fig. 4E-O), although expression of *pea3* and *dusp6* is already weakly reduced in *fgf10/dae* at 28 hpf (Fig. 4E,F,L,M). We then analysed markers of the dorsoventral (DV) axis expressed in the ectoderm, which might depend on Fgf10 signalling from the underlying mesenchyme. The expression of *eng1a* in the ventral ectoderm is weakly reduced at 28 hpf (Fig. 5A,B), but virtually absent by 38 hpf (Fig. 5C,D). We also examined the expression of zebrafish *wnt7a*, which is expressed in the dorsal ectoderm, as observed

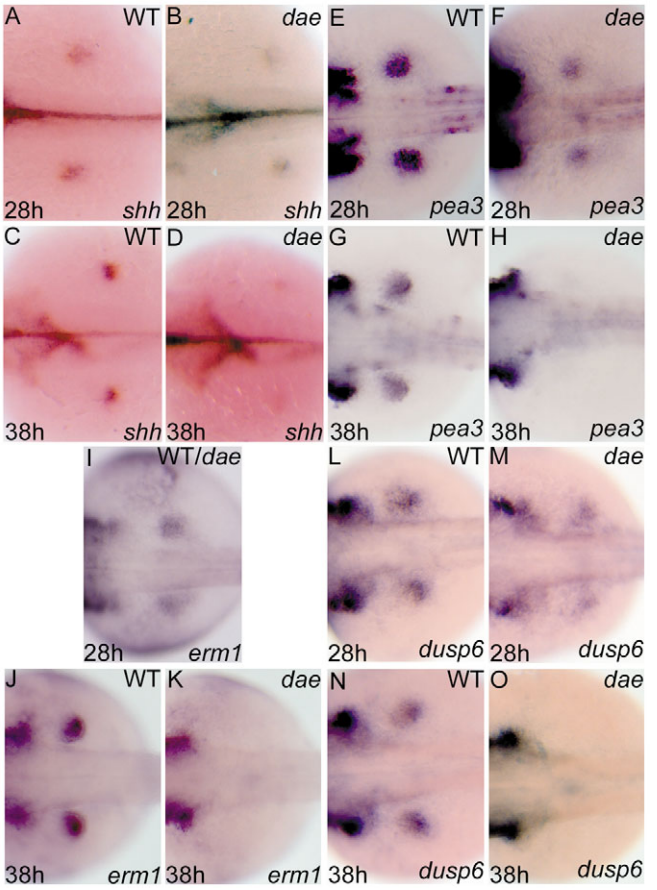

Fig. 4. Expression of AER target genes is reduced in *fgf10/dae*. Dorsal views of in situ hybridisation staining of wild-type (A,C,E,G,J,L,N) and mutant embryos (B,D,F,H,K,M,O) with anterior towards the left. At 28 hpf, expression of all genes analysed appears either indistinguishable between *fgf10/dae* and sibling (I), or weakly reduced in mutant (B,F,M). By 38 hpf, expression of ridge target genes appear either strongly reduced (D) or absent (H,K,O) in *fgf10/dae*.

in other vertebrate species (Capdevila and Izpisua Belmonte, 2001). We find that, similar to *eng1a*, *wnt7a* expression is present in *fgf10/dae* mutants at 28 hpf (Fig. 5E,F), but is absent at 38 hpf (Fig. 5G,H). Together, these results indicate that Fgf-dependent marker gene expression is initially established in zebrafish *fgf10* mutants, but is lost by around 36 hpf of development. Similarly, expression of *eng1a* in the ventral ectoderm, and *wnt7a* in the dorsal ectoderm is initiated normally in the absence of Fgf10, but is subsequently downregulated.

Zebrafish *ext2/dak* and *extl3/box* mutants have pectoral fin phenotypes similar to *fgf10/dae* mutants

The *fgf10/dae* pectoral fin phenotype described here is similar to that of the zebrafish *dackel* (*dak*) mutant (Grandel et al., 2000), which has recently been shown to disrupt the *ext2* gene (Lee et al., 2004). The zebrafish *boxer* (*box*) mutant disrupts *extl3*, another *exostosin* family member and shares several phenotypes with *ext2/dak* (van Eeden et al., 1996; Lee et al., 2004). Therefore, we compared the pectoral fin phenotype of *extl3/box* to that of *ext2/dak* and *dae* in more detail. At early

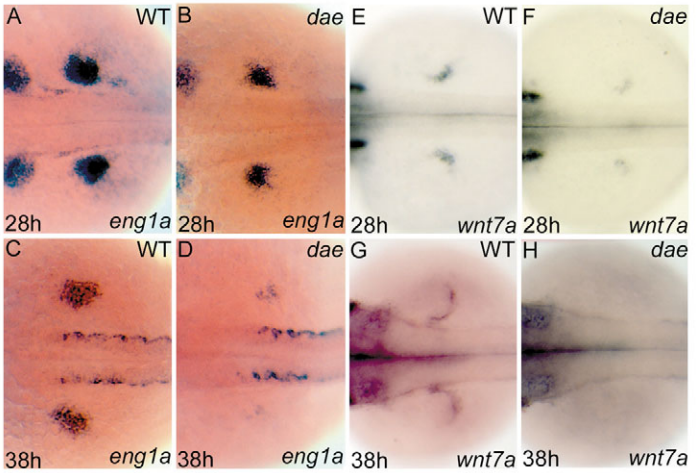

Fig. 5. Expression of DV axis markers is disrupted in *fgf10/dae*. Dorsal views of in situ hybridisation staining of wild-type (A,C,E,G) and *fgf10/dae* (B,D,F,H) embryos. Expression of all genes analysed appears slightly reduced at 28 hpf in *fgf10/dae* (B,F) when compared with siblings (A,E). By 38 hpf, *eng1a* expression is severely reduced (D) and *wnt7a* expression (H) is absent in *fgf10/dae*.

developmental stages (28 hpf), *ext2/dak* mutants show only very weak effects on fin development, and strongly resemble wild-type siblings (Grandel et al., 2000). We find that *extl3/box* mutants show even weaker phenotypes at this stage and are virtually indistinguishable from wild-type siblings (data not shown). At 48 hpf, we find that expression of the AER markers *dlx2a* and *fgf8* is strongly reduced in *extl3/box* mutants (Fig. 6A,B,D,E). Similarly, expression of the Fgf-dependent marker *shh*, and the expression of *eng1a* is reduced in *extl3/box* mutants at this stage (Fig. 6G,H,J,K). The reduction of these markers is not as severe as in *fgf10/dae* or in *ext2/dak* mutants (Fig. 6C,F,I,L), but the phenotype of *extl3/box* mutants is more variable than that of the other two mutants. In a few strongly affected *extl3/box* mutants, marker gene reduction is as severe as in *fgf10/dae* or in *ext2/dak* mutants (data not shown). These results indicate that *extl3/box* has a similar, although on average weaker, phenotype to *fgf10/dae* and *ext2/dak*, thus raising the possibility that these three genes function in the same pathway.

Removal of one copy of *fgf10/dae* strongly enhances the *extl3/box* limb phenotype

To further explore the possibility that Fgf10 and Extl3 function in the same genetic pathway, we crossed the *fgf10/dae* mutation into the *extl3/box* mutant background. As the *extl3/box* phenotype is weaker than that of the *fgf10/dae* and *ext2/dak* mutants, we reasoned that a low level of Fgf10 signalling is retained in *extl3/box* mutants. If so, further reduction of Fgf10 signalling, by reducing the level of Fgf10 protein through genetic removal of one copy of the *fgf10/dae* gene, should cause an enhancement of the *extl3/box* phenotype (Fig. 7). Indeed, we observe that $box^{-/-};dae^{+/-}$ larvae have a much stronger pectoral fin reduction than *box* mutants alone, resembling *fgf10/dae* or *ext2/dak* mutants in severity (Fig. 7E). We identified double mutants both on the basis of their much severer phenotype (73 out of 150, or 49% of total mutants scored, corresponding to the expected Mendelian ratio) and by

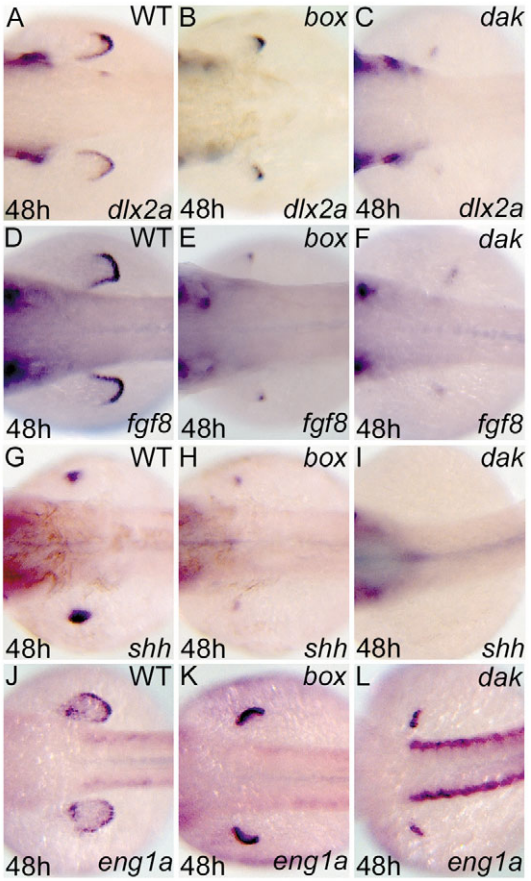

Fig. 6. Expression of fin marker genes compared in *extl3/box* and *ext2/dak* mutants. In situ hybridisation staining of wild-type (A,D,G,J), *extl3/box* (B,E,H,K) and *ext2/dak* (C,F,I,L) embryos. All panels are dorsal views with anterior towards the left. At 48 hpf, *extl3/box* mutant embryos have reduced expression of all markers analysed (B,E,H,K) when compared with wild type (A,D,G,J). *ext2/dak* mutants have a stronger phenotype. There is a strong reduction of *dlx2a* (C), *fgf8* (F) and *eng1a* (L). Expression of *shh* is absent in *ext2/dak* (I) by 48 hpf of development.

SNP genotyping (Fig. 7F). Following PCR amplification and digestion with *Taq1*, *extl3/box* larvae with a strong reduction of fin tissue were confirmed to be $dae^{+/-}$ by the presence of two bands visible on an agarose gel. This strong genetic interaction between *extl3* and *fgf10* during limb development further indicates that these genes act in the same pathway.

AER-derived Fgf4 activates *eng1a* and *wnt7a* in the ectoderm

Our data indicate that *fgf10/dae* activity is necessary for maintenance of *eng1a* expression in the ventral ectoderm. However, as Fgf10 signalling also activates *fgf4* and *fgf8* expression in the AER, it is presently not clear if *eng1a* depends directly on Fgf10 from the underlying mesenchyme, or if it instead depends on Fgf4/8 signalling from the AER. In order to distinguish between these possibilities, we performed gain-of-function experiments by applying either Fgf10 or Fgf4 protein to *fgf10/dae* mutant limb buds. We find that implantation of Fgf10-soaked beads into *fgf10/dae* mutants results in the rescue of *fgf8* expression in the AER (4 out of 7

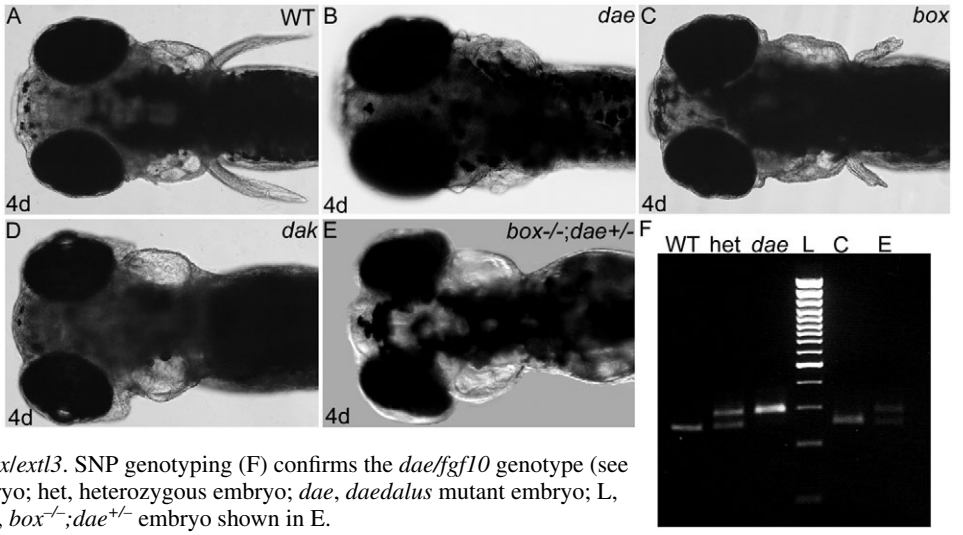

Fig. 7. A strong genetic interaction between *fgf10/dae* and *extl3/box* during limb development. Four-day live photos (A-E) of wild-type (A), *fgf10/dae* (B), *extl3/box* (C), *ext2/dak* (D) and *box*$^{-/-}$;*dae*$^{+/-}$ (E) embryos. All photos are dorsal views with anterior towards the left. *dae* (B) mutant embryos have a severe truncation of pectoral fin compared with siblings (A). *extl3/box* (C) mutants have a weaker pectoral fin truncation, whereas *ext2/dak* (D) appears similar to *fgf10/dae* and has a severe truncation of the fin. Removal of one copy of *fgf10* in an *extl3/box* mutant background (E) severely worsens the *extl3/box* phenotype, demonstrating a genetic interaction between *dae/fgf10* and *box/extl3*. SNP genotyping (F) confirms the *dae/fgf10* genotype (see Materials and methods). WT, wild-type embryo; het, heterozygous embryo; *dae*, *daedalus* mutant embryo; L, ladder; C, *box* mutant embryo shown in C; E, *box*$^{-/-}$;*dae*$^{+/-}$ embryo shown in E.

dae; Fig. 8A). This treatment also rescues *shh* expression in the posterior mesenchyme (5 out of 5 *dae*; Fig. 8B), *eng1a* expression in the ventral ectoderm (4 of 7 *dae*: Fig. 8C) and *wnt7a* in dorsal ectoderm (5 out of 5 *dae*: Fig. 8D) of *fgf10/dae* mutant limb buds. Implantation of control beads soaked in PBS has no effect on mutant limb buds (Fig. 8E). Interestingly, implantation of Fgf4-soaked beads also leads to rescue of *shh* (6 out of 9 *dae*; Fig. 9B), *eng1a* (8 out of 11 *dae*; Fig. 9C) and *wnt7a* (3 out of 3 *dae*; data not shown) expression in *fgf10/dae* mutants, but is unable to rescue *fgf8* expression (0 out of 6 *dae*; Fig. 9A). These results indicate that Fgf4 is able to activate *eng1a* in the absence of *fgf10* activity, suggesting that the effect of *fgf10* on *eng1a* expression is mediated by the activation of *fgf4* expression in the AER.

Failure of *ext2/dak* mutant limb buds to activate target gene expression in response to Fgf10 protein

Since *ext2/dak*, *extl3/box* and *fgf10/dae* all show a similar disruption of the AER during pectoral fin development, this raises the possibility that HSPG synthesis by Ext2 and Extl3 is necessary for Fgf10 signalling. To test this hypothesis directly, we implanted Fgf10-soaked beads into both *ext2/dak* and *extl3/box* mutant limb buds. We compared the effect of this treatment to that of Fgf4 soaked beads, which have previously been shown to activate several target genes in *ext2/dak* mutants (Grandel et al., 2000). We find that implantation of Fgf10 soaked beads into either *ext2/dak* or *extl3/box* mutant limb buds fails to rescue expression of *fgf8* (0 out of 5 *dak*; Fig. 10A), *shh* (0 out of 9 *dak*; Fig. 10B; 0 out of 3 *box*; Fig. 10E), *eng1a* (0 out of 4 *dak*; Fig. 10C) or *wnt7a* (0 out of 3 *dak*; Fig. 10D), whereas implantation of the same batch of beads into *fgf10/dae* mutant embryos does lead to activation of these markers (Fig. 8; data not shown). By contrast, implantation of Fgf4-soaked beads is able to rescue expression of all genes analysed: *eng1a* (3 out of 4 *dak*; Fig. 11A), *wnt7a* (4 out of 4 *dak*; Fig. 11B)

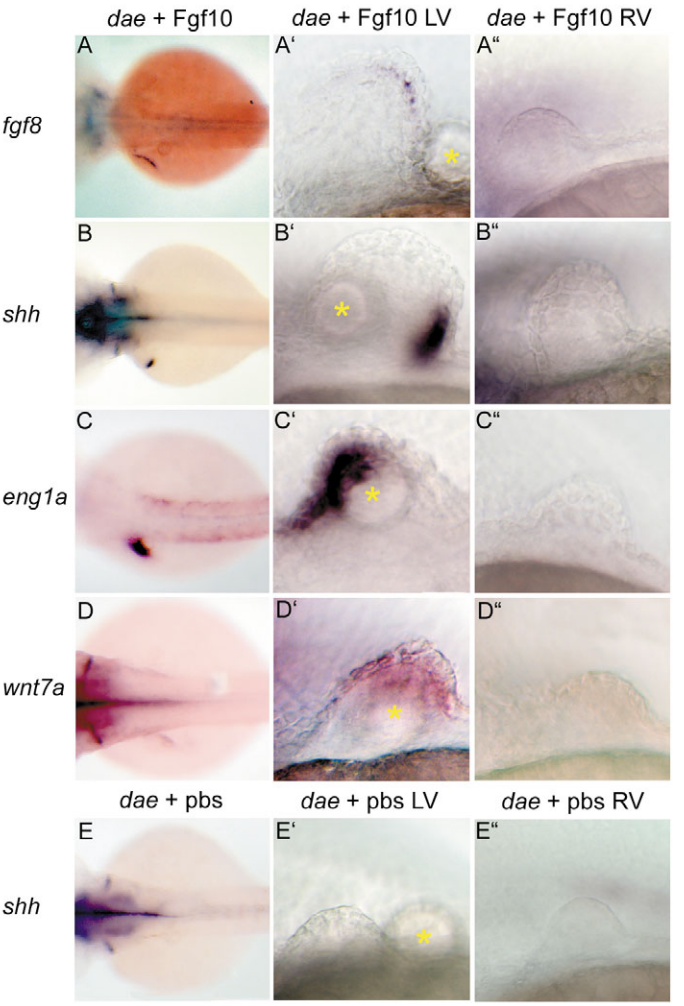

Fig. 8. Implantation of Fgf10 soaked beads into *fgf10/dae* mutant fin buds. Dorsal (A-E) and lateral (A′-E′′) views of 2.5-day-old embryos with anterior towards the left. Fgf10 protein rescues expression of *fgf8* (A-A′′), *shh* (B-B′′), *eng1a* (C-C′′) and *wnt7a* (D-D′′) following bead implantation into the left-hand side fin bud (A′-D′) when compared with unoperated right-hand side fin buds (A′′-D′′). Yellow asterisks mark position of implanted beads (A′-E′). As a control, implantation of beads soaked in PBS (E-E′′) does not rescue marker gene expression. LV, left view of embryo; RV, right view of same embryo.

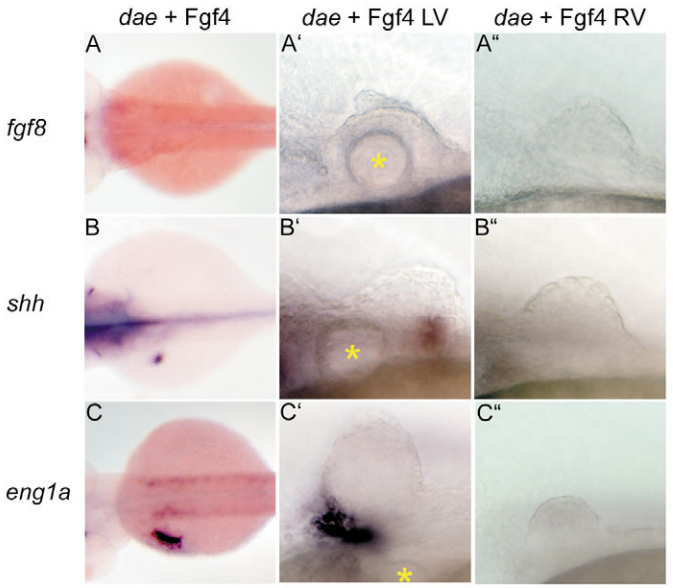

Fig. 9. Implantation of Fgf4 protein-soaked beads into *fgf10/dae* fin buds. Dorsal (A-C) and lateral (A′-C′′) views of 2.5-day-old embryos, anterior towards the left. Expression of genes indicated was examined by in situ hybridisation in operated left-hand side (A′-C′) and unoperated right hand side fin buds (A′′-C′′). Fgf4 protein is unable to rescue expression of *fgf8* (A-A′′). Conversely, Fgf4 protein is able to rescue the expression of both *shh* (B-B′′) and *eng1a* (C-C′′) in operated fin buds. Yellow asterisks indicate the position of implanted beads (A′-C′). LV, left view of embryo; RV, right view of same embryo.

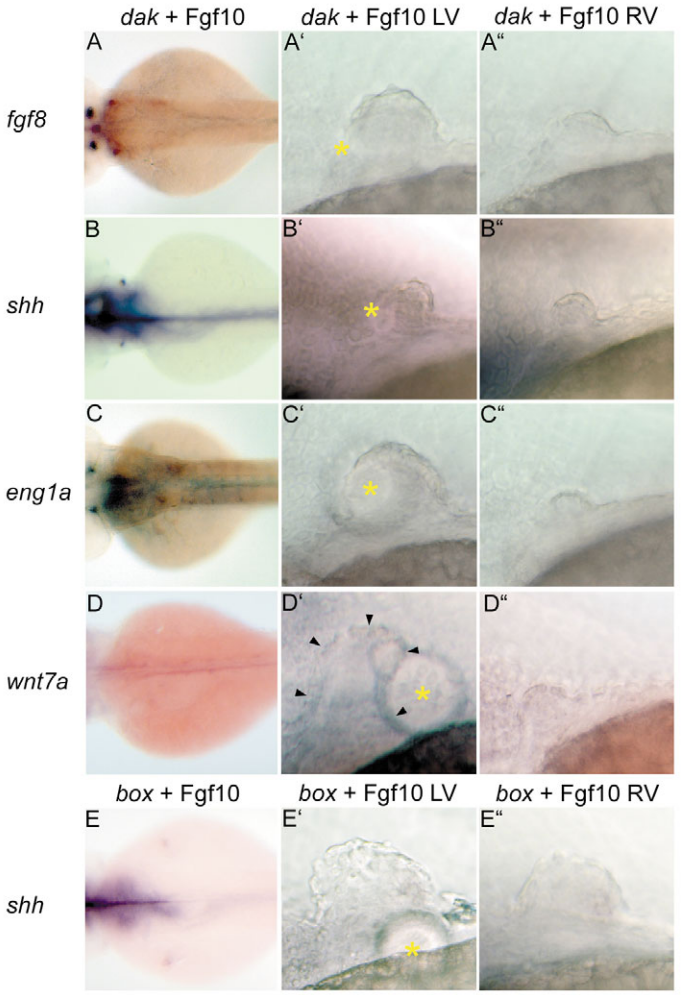

Fig. 10. Implantation of Fgf10-soaked beads into *ext2/dak* and *extl3/box* embryos. Dorsal (A-E) and lateral (A′-E′′) views of 2.5-day-old embryos, anterior towards the left. Expression of genes indicated was examined by in situ hybridisation in operated left-hand side (A′-E′) and unoperated right-hand side fin buds (A′′-E′′) *dak* fin buds. Implantation of Fgf10 protein-soaked beads into *extl3/box* also fails to rescue the expression of *shh* (E′). Yellow asterisks indicate position of implanted beads (A′-E′). LV, left view of embryo; RV, right view of same embryo.

and *shh* (5 out of 5 *box*; Fig. 11C) in *ext2/dak* or *extl3/box* mutant limb buds. Collectively, these results indicate that HSPG synthesis by Ext2 and Extl3 is required for Fgf10, but not for Fgf4, signalling.

Discussion

Zebrafish *fgf10* is crucial for AER development

In this study, we have shown that the *daedalus* mutation disrupts zebrafish *fgf10* and that, in the absence of *fgf10* activity, development of the pectoral fin bud is severely compromised. Our analysis suggests that some early steps in fin development appear to be intact in *fgf10/dae* mutants. Three observations support this conclusion: first, a pectoral fin bud with a small apical thickening is present in *fgf10/dae* mutants, which gives rise to proximal endoskeletal elements (Fig. 1). This is in contrast to the *fgf24* mutant, in which the bud fails to grow out at all, and no endoskeletal elements are formed. Second, several early AER markers, including *bmp2b* and *sp8* (Fig. 3), are initially activated in *fgf10/dae* mutants, albeit at reduced levels, and are subsequently lost. Third, the expression of both ZPA markers and Fgf target genes, such as *shh*, *pea3*, *erm1* and *dusp6* (Fig. 4), is initiated in the absence of Fgf10, and then lost later on indicating that initiation of Fgf signalling occurs normally in the absence of *fgf10* activity.

As AER expression of *sp8* and *bmp2b* is already reduced in *fgf10* mutants at early stages, our results suggest that *fgf10* contributes to initial AER induction, and is then uniquely required for AER maintenance. In agreement with this, the majority of AER expressed genes we examined (including *sp9*, *dlx2a* and *wnt3l*) were strongly reduced by 28 hpf. The early expression of *shh* and Fgf target genes in the zebrafish may thus be independent of the AER, and might instead be directed by Fgf24 in the mesenchyme. This would be in contrast to the situation in tetrapods, where *shh* activation depends on the AER from the very beginning.

The *daedalus* phenotype appears to be weaker than that of mouse *Fgf10* mutants, in which the AER is never established, and ZPA marker genes such as *shh* fail to be activated (Min et al., 1998; Sekine et al., 1999). These observations suggest that the early and late roles played by Fgf10 in the mouse, i.e. initial AER induction, followed by subsequent AER maintenance, are regulated differently in the zebrafish: initial AER induction is directed by *fgf10* plus a second gene, whereas AER maintenance depends entirely on *fgf10*. In this respect, *fgf10*

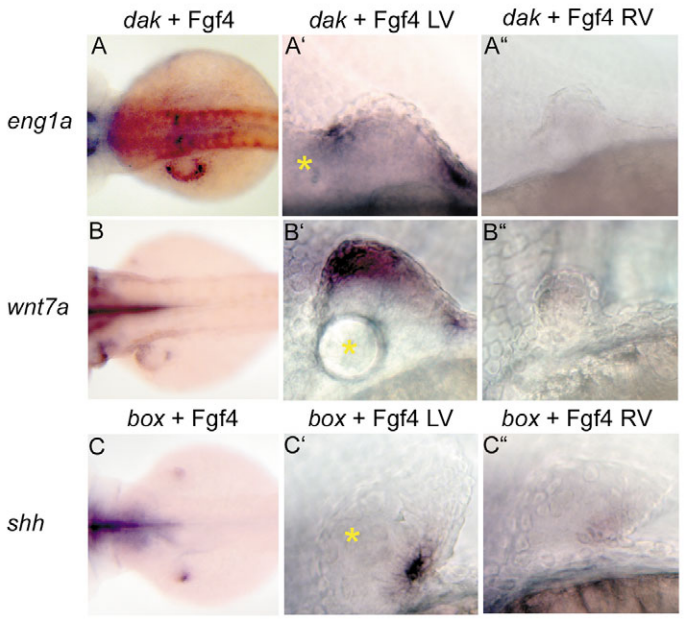

Fig. 11. Implantation of Fgf4-soaked beads into *ext2/dak* and *extl3/box* embryos. Dorsal (A-C) and lateral (A′-C′′) views of 2.5-day-old embryos, anterior towards the left. Expression of genes was examined by in situ hybridisation in operated left-hand side (A′-C′) and unoperated right-hand side fin buds (A′′-C′′). Fgf4 protein beads strongly rescued the expression of *eng1a* (A-A′′) and *wnt7a* (B-B′′) in *ext2/dak* mutant embryos. Similarly, *shh* (C-C′′) expression was rescued in *extl3/box* following implantation of Fgf4-soaked beads. Yellow asterisks indicate position of implanted beads (A′-C′). LV, left view of embryo; RV, right view of same embryo.

acts as a classical apical ectodermal maintenance factor (AEMF) (Zwilling et al., 1959; Ohuchi et al., 1997).

If *fgf10* is not uniquely required for AER induction, what is the nature of the additional AER-inducing signal in zebrafish? An in silico search of the zebrafish genome did not reveal a second *fgf10* orthologue (W.H.J.N., unpublished), suggesting that redundancy following duplication cannot explain this phenotype. Previous results indicate that *fgf24* may provide this function (Fischer et al., 2003). Zebrafish *fgf24* mutants show no morphological sign of pectoral fin bud formation, have no apical thickening and fail to activate expression of any AER markers. The expression of *fgf24* is present in the lateral plate mesoderm prior to that of *fgf10*, and *fgf10* expression is dependent on *fgf24* activity (Fischer et al., 2003). Furthermore, activation of *fgf24* expression is not dependent on *fgf10* activity (Fig. 3). The complete absence of pectoral fin buds in *fgf24* mutants raises the issue of whether fin bud development is initiated at all in the absence of *fgf24*. The normal initial activation of *tbx5* and *msxc* expression in the lateral plate mesoderm *fgf24* mutants, however, indicates that these cells have been correctly specified as early limb bud cells, but that subsequent relay of the limb inducing signal to the ectoderm fails in the absence of *fgf24* (Fischer et al., 2003).

Intriguingly, no *fgf24* orthologue is present in tetrapod genomes, although it can be found in sharks (Draper et al., 2003). As sharks diverged from the ancestors of teleosts before tetrapods, this suggests that *fgf24* was initially present, but then lost during the evolution of land vertebrates. To allow for this loss, other Fgf genes must have taken over the function of *fgf24* in tetrapods. These Fgf genes include *fgf8* during posterior mesoderm development (Draper et al., 2003), and *fgf10* during early limb development (Fischer et al., 2003) (this study).

Fgf4 directs *wnt7a* and *eng1a* expression in the ectoderm

Our data demonstrate that expression of *eng1a* and *wnt7a*, respective markers of the ventral and dorsal limb ectoderm, depend on Fgf10 signalling as they are lost in *fgf10/dae* mutants. However, as AER signalling is also abrogated in these mutants, it is not clear how direct this effect is. Our gain-of-function experiments show that Fgf4, which is expressed in the AER, can rescue both *eng1a* and *wnt7a* expression in the absence of *fgf10/dae* activity. Although we cannot exclude the possibility that Fgf10 also activates these genes directly, our results show that failure of Fgf4 signalling from the AER is sufficient to explain why *eng1a* and *wnt7a* are lost in *fgf10* mutants. This implies that the effect of Fgf10 signalling on *eng1a* and *wnt7a* expression is mediated by activation of *fgf4* expression in the AER, which in turn signals to dorsal and ventral ectoderm. Fgf4 protein is unable to rescue *fgf8* expression in the AER of *fgf10/dae* mutants, consistent with the proposal that mesenchymal Fgf10 signals to the overlying AER through Fgfr2b, whereas Fgf4 signals through Fgfr2c. Thus, our results confirm that Fgf4 is unable to replace Fgf10 signalling to the AER, and indicate that this response can only be triggered via Fgf10. It remains to be determined through which receptor Fgf4 activates *wnt7a* and *eng1a* expression in the ectoderm.

HSPG synthesis by Ext2 and Extl3 is required for Fgf10 signalling during limb development

We have shown here that the failure of AER maintenance in *fgf10/dae* mutants is very similar to that previously described in *ext2/dak* mutants (Grandel et al., 2000). In addition, we have shown that *extl3/box* mutants have similar defects in AER maintenance, although their phenotype is weaker than that of the other two mutants. These results suggest that these three genes act in the same pathway required for AER maintenance. This proposal is further supported by the observation that genetic removal of one copy of *fgf10/dae* dramatically enhances the severity of the *extl3/box* phenotype. The weaker phenotype of *extl3/box* mutants correlates well with the observation that *extl3/box* mutants have a weaker reduction of HS levels than *ext2/dak* mutants (Lee et al., 2004). As Ext2 and Extl3 are required for the polymerisation of HS side chains on HSPGs, these results suggest that HSPG synthesised by Ext2 and Extl3 is required for Fgf10 function. Our gain-of-function data provide direct evidence for this possibility, as application of Fgf10 protein is able to rescue target gene expression in *fgf10/dae* mutants, but not in *ext2/dak* or *extl3/box* mutants. Furthermore, transplantation of wild-type cells into the epidermis of *ext2/dak* fin buds has been shown to enable a local rescue of AER development (Grandel et al., 2000). Taken together, these results suggest that HSPG synthesis by Ext2 and Extl3 in the fin bud ectoderm is required for ectodermal cells to respond to Fgf10 protein secreted by the underlying mesenchyme.

Specificity of HSPGs in modulating signalling by distinct signalling factors

The pectoral fin phenotype of *ext2/dak* and *extl3/box* mutants strongly resembles that of *fgf10/dae* mutants, but not that of *fgf24* mutants. Therefore, HSPGs appear to be differentially required for Fgf10 signalling during limb development. In direct support of this proposal, we find that both *ext2/dak* and *extl3/box* mutants are able to respond to application of Fgf4 protein, but are unable to respond to Fgf10 protein. This agrees well with the observation that distinct Fgfs differ in the amino acid composition of their heparin-binding residues (Bellosta et al., 2001). Taken together, these results indicate that distinct Fgfs have different requirements for HS in vivo.

Interestingly, both Fgf4 and Fgf24 belong to the subgroup of Fgf ligands with preference for Fgfr2c, whereas Fgf10 belongs to the subgroup with preference for Fgfr2b (Orr-Urtreger et al., 1993; Ornitz et al., 1996; Fischer et al., 2003), raising the possibility that these classes of Fgfs may have differential requirements for HS in vivo. Alternatively, the different receptor subtypes might determine the role played by HS during receptor binding and activation. Arguing against this hypothesis is the observation that conditional removal of Ext1 activity from the mouse CNS results in several phenotypes that may be caused by abrogated Fgf8 signalling (Inatani et al., 2003), as Fgf8 also signals preferentially through Fgfr2c. Another possibility could be that Fgf signalling to the mesenchyme might be much less HSPG dependent than signalling to the ectoderm. This is unlikely, however, given that Fgf4 can activate ectodermal *eng1a* and *wnt7a* expression in *ext2/dak* mutants.

The *Drosophila* Exostosin genes have been shown to be crucial for Hh distribution and signalling during imaginal disc development (reviewed by Nybakken and Perrimon, 2002; Lin, 2004). Similarly, mouse mutations in Ext1 affect Ihh distribution and signalling (Lin et al., 2000; Koziel et al., 2004). It is therefore surprising that none of the phenotypes of *ext2/dak* and *extl3/box* can be linked to Hh signalling. During limb development, signalling by Shh is clearly not affected in these mutants, as rescue of Shh expression in *ext2/dak* mutant fin buds, by application of Fgf4 beads, leads to normal activation of the Hh dependent target genes *hoxd11* and *hoxd13* (Grandel et al., 2000).

Although it is possible that some signalling factors do not require the presence of any HSPGs for their function, at least in some cellular contexts, an alternative possibility is that different factors require different levels of HSPGs in different contexts. As overall HS levels are strongly reduced, but not absent, in *ext2/dak* and *extl3/box* mutants (Lee et al., 2004), this might be an indication that signalling by Fgf10 requires much higher levels of HS than other signalling events during limb development.

Taken together, these results indicate that the effect of HSPGs on cell-cell signalling is both signal and context dependent. This provides an explanation of why the phenotypes of *ext2/dak* and *extl3/box* mutants are so discrete and specific, even though both genes are broadly expressed (Lee et al., 2004), and their disruption causes a global reduction of HS levels. Because of this specificity in the control of developmental signalling by HSPGs, it will be critical to identify the exact signalling factors modulated by HSPGs in different organs and cell types in vivo, in order to better understand the biological relevance of this mechanism of signal regulation.

We thank Katherine Brown, Gillian Brunt, Filippo Del Bene, David Hipfner, Nadia Mercader, Maria Sakkou and Valia Stamataki for critically reading an earlier version of the manuscript, and members of the Neumann and Wittbrodt groups for stimulating discussions. The Wnt sequence alignments were assembled with help from Aidan Budd. *wnt3l* was a generous gift from Dr Arne Lekven. We thank Sabine Fischer and Gillian Brunt for excellent technical assistance and fish room care. J.L. is funded by the Swedish SSF through the EMBL Alumni Association.

Supplementary material

Supplementary material for this article is available at
http://dev.biologists.org/cgi/content/full/132/22/4963/DC1

References

Akimenko, M. A., Ekker, M., Wegner, J., Lin, W. and Westerfield, M. (1994). Combinatorial expression of three zebrafish genes related to distal-less: part of a homeobox gene code for the head. *J. Neurosci.* **14**, 3475-3486.

Bellosta, P., Iwahori, A., Plotnikov, A. N., Eliseenkova, A. V., Basilico, C. and Mohammadi, M. (2001). Identification of receptor and heparin binding sites in fibroblast growth factor 4 by structure-based mutagenesis. *Mol. Cell. Biol.* **21**, 5946-5957.

Bornemann, D. J., Duncan, J. E., Staatz, W., Selleck, S. and Warrior, R. (2004). Abrogation of heparan sulfate synthesis in Drosophila disrupts the Wingless, Hedgehog and Decapentaplegic signaling pathways. *Development* **131**, 1927-1938.

Capdevila, J. and Izpisua Belmonte, J. C. (2001). Patterning mechanisms controlling vertebrate limb development. *Annu. Rev. Cell Dev. Biol.* **17**, 87-132.

Castresana, J. (2000). Selection of conserved blocks from multiple alignments for their use in phylogenetic analysis. *Mol. Biol. Evol.* **17**, 540-552.

Draper, B. W., Morcos, P. A. and Kimmel, C. B. (2001). Inhibition of zebrafish fgf8 pre-mRNA splicing with morpholino oligos: a quantifiable method for gene knockdown. *Genesis* **30**, 154-156.

Draper, B. W., Stock, D. W. and Kimmel, C. B. (2003). Zebrafish fgf24 functions with fgf8 to promote posterior mesodermal development. *Development* **130**, 4639-4654.

Ekker, M., Wegner, J., Akimenko, M. A. and Westerfield, M. (1992). Coordinate embryonic expression of three zebrafish engrailed genes. *Development* **116**, 1001-1010.

Esko, J. D. and Selleck, S. B. (2002). Order out of chaos: assembly of ligand binding sites in heparan sulfate. *Annu. Rev. Biochem.* **71**, 435-471.

Fischer, S., Draper, B. W. and Neumann, C. J. (2003). The zebrafish fgf24 mutant identifies an additional level of Fgf signaling involved in vertebrate forelimb initiation. *Development* **130**, 3515-3524.

Garcia-Garcia, M. J. and Anderson, K. V. (2003). Essential role of glycosaminoglycans in Fgf signaling during mouse gastrulation. *Cell* **114**, 727-737.

Grandel, H. and Schulte-Merker, S. (1998). The development of the paired fins in the zebrafish (Danio rerio). *Mech. Dev.* **79**, 99-120.

Grandel, H., Draper, B. W. and Schulte-Merker, S. (2000). dackel acts in the ectoderm of the zebrafish pectoral fin bud to maintain AER signaling. *Development* **127**, 4169-4178.

Habeck, H., Odenthal, J., Walderich, B., Maischein, H. and Schulte-Merker, S. (2002). Analysis of a zebrafish VEGF receptor mutant reveals specific disruption of angiogenesis. *Curr. Biol.* **12**, 1405-1412.

Han, C., Belenkaya, T. Y., Khodoun, M., Tauchi, M. and Lin, X. (2004). Distinct and collaborative roles of Drosophila EXT family proteins in morphogen signalling and gradient formation. *Development* **131**, 1563-1575.

Humphrey, C. D. and Pittman, F. E. (1974). A simple methylene blue-azure II-basic fuchsin stain for epoxy-embedded tissue sections. *Stain Technol.* **49**, 9-14.

Inatani, M., Irie, F., Plump, A. S., Tessier-Lavigne, M. and Yamaguchi, Y. (2003). Mammalian brain morphogenesis and midline axon guidance require heparan sulfate. *Science* **302**, 1044-1046.

Itoh, N. and Ornitz, D. M. (2004). Evolution of the Fgf and Fgfr gene families. *Trends Genet.* **20**, 563-569.
Johnson, R. L. and Tabin, C. J. (1997). Molecular models for vertebrate limb development. *Cell* **90**, 979-990.
Kawakami, Y., Rodriguez-Leon, J., Koth, C. M., Buscher, D., Itoh, T., Raya, A., Ng, J. K., Esteban, C. R., Takahashi, S., Henrique, D. et al. (2003). MKP3 mediates the cellular response to FGF8 signalling in the vertebrate limb. *Nat. Cell Biol.* **5**, 513-519.
Kawakami, Y., Esteban, C. R., Matsui, T., Rodriguez-Leon, J., Kato, S. and Belmonte, J. C. (2004). Sp8 and Sp9, two closely related buttonhead-like transcription factors, regulate Fgf8 expression and limb outgrowth in vertebrate embryos. *Development* **131**, 4763-4774.
Koziel, L., Kunath, M., Kelly, O. G. and Vortkamp, A. (2004). Ext1-dependent heparan sulfate regulates the, range, of, Ihh signaling during endochondral ossification. *Dev. Cell* **6,** 801-813.
Krauss, S., Korzh, V., Fjose, A. and Johansen, T. (1992). Expression of four zebrafish wnt-related genes during embryogenesis. *Development* **116**, 249-259.
Krauss, S., Concordet, J. P. and Ingham, P. W. (1993). A functionally conserved homolog of the Drosophila segment polarity gene hh is expressed in tissues with polarizing activity in zebrafish embryos. *Cell* **75**, 1431-1444.
Lee, J. S., von der Hardt, S., Rusch, M. A., Stringer, S. E., Stickney, H. L., Talbot, W. S., Geisler, R., Nusslein-Volhard, C., Selleck, S. B., Chien, C. B. et al. (2004). Axon sorting in the optic tract requires HSPG synthesis by ext2 (dackel) and extl3 (boxer). *Neuron* **44**, 947-960.
Lin, X. (2004). Functions of heparan sulfate proteoglycans in cell signaling during development. *Development* **131**, 6009-6021.
Lin, X., Buff, E. M., Perrimon, N. and Michelson, A. M. (1999). Heparan sulfate proteoglycans are essential for FGF receptor signaling during Drosophila embryonic development. *Development* **126**, 3715-3723.
Lin, X., Wei, G., Shi, Z., Dryer, L., Esko, J. D., Wells, D. E. and Matzuk, M. M. (2000). Disruption of gastrulation and heparan sulfate biosynthesis in EXT1-deficient mice. *Dev. Biol.* **224**, 299-311.
Macdonald, R., Xu, Q., Barth, K. A., Mikkola, I., Holder, N., Fjose, A., Krauss, S. and Wilson, S. W. (1994). Regulatory gene expression boundaries demarcate sites of neuronal differentiation in the embryonic zebrafish forebrain. *Neuron* **13**, 1039-1053.
Martin, G. R. (1998). The roles of FGFs in the early development of vertebrate limbs. *Genes Dev* **12**, 1571-86.
Martinez-Barbera, J. P., Toresson, H., Da Rocha, S. and Krauss, S. (1997). Cloning and expression of three members of the zebrafish Bmp family: Bmp2a, Bmp2b and Bmp4. *Gene* **198**, 53-59.
Min, H., Danilenko, D. M., Scully, S. A., Bolon, B., Ring, B. D., Tarpley, J. E., DeRose, M. and Simonet, W. S. (1998). Fgf-10 is required for both limb and lung development and exhibits striking functional similarity to Drosophila branchless. *Genes Dev.* **12**, 3156-3161.
Ng, J. K., Kawakami, Y., Buscher, D., Raya, A., Itoh, T., Koth, C. M., Rodriguez Esteban, C., Rodriguez-Leon, J., Garrity, D. M., Fishman, M. C. et al. (2002). The limb identity gene Tbx5 promotes limb initiation by interacting with Wnt2b and Fgf10. *Development* **129**, 5161-5170.
Nybakken, K. and Perrimon, N. (2002). Heparan sulfate proteoglycan modulation of developmental signaling in Drosophila. *Biochim. Biophys. Acta* **1573**, 280-291.
Ohuchi, H., Nakagawa, T., Yamamoto, A., Araga, A., Ohata, T., Ishimaru, Y., Yoshioka, H., Kuwana, T., Nohno, T., Yamasaki, M. et al. (1997). The mesenchymal factor, FGF10, initiates and maintains the outgrowth of the chick limb bud through interaction with FGF8, an apical ectodermal factor. *Development* **124**, 2235-2244.
Ornitz, D. M. (2000). FGFs, heparan sulfate and FGFRs: complex interactions essential for development. *BioEssays* **22**, 108-112.
Ornitz, D. M., Xu, J., Colvin, J. S., McEwen, D. G., MacArthur, C. A., Coulier, F., Gao, G. and Goldfarb, M. (1996). Receptor specificity of the fibroblast growth factor family. *J. Biol. Chem.* **271**, 15292-15297.
Orr-Urtreger, A., Bedford, M. T., Burakova, T., Arman, E., Zimmer, Y., Yayon, A., Givol, D. and Lonai, P. (1993). Developmental localization of the splicing alternatives of fibroblast growth factor receptor-2 (FGFR2). *Dev. Biol.* **158**, 475-486.
Pellegrini, L., Burke, D. F., von Delft, F., Mulloy, B. and Blundell, T. L. (2000). Crystal structure of fibroblast growth factor receptor ectodomain bound to ligand and heparin. *Nature* **407**, 1029-1034.
Reifers, F., Bohli, H., Walsh, E. C., Crossley, P. H., Stainier, D. Y. and Brand, M. (1998). Fgf8 is mutated in zebrafish acerebellar (ace) mutants and is required for maintenance of midbrain-hindbrain boundary development and somitogenesis. *Development* **125**, 2381-2395.
Roehl, H. and Nusslein-Volhard, C. (2001). Zebrafish pea3 and erm are general targets of FGF8 signaling. *Curr. Biol.* **11**, 503-507.
Schlessinger, J., Plotnikov, A. N., Ibrahimi, O. A., Eliseenkova, A. V., Yeh, B. K., Yayon, A., Linhardt, R. J. and Mohammadi, M. (2000). Crystal structure of a ternary FGF-FGFR-heparin complex reveals a dual role for heparin in FGFR binding and dimerization. *Mol. Cell* **6**, 743-750.
Sekine, K., Ohuchi, H., Fujiwara, M., Yamasaki, M., Yoshizawa, T., Sato, T., Yagishita, N., Matsui, D., Koga, Y., Itoh, N. et al. (1999). Fgf10 is essential for limb and lung formation. *Nat. Genet.* **21**, 138-141.
Sun, X., Mariani, F. V. and Martin, G. R. (2002). Functions of FGF signalling from the apical ectodermal ridge in limb development. *Nature* **418**, 501-508.
Takei, Y., Ozawa, Y., Sato, M., Watanabe, A. and Tabata, T. (2004). Three Drosophila EXT genes shape morphogen gradients through synthesis of heparan sulfate proteoglycans. *Development* **131**, 73-82.
The, I., Bellaiche, Y. and Perrimon, N. (1999). Hedgehog movement is regulated through tout velu-dependent synthesis of a heparan sulfate proteoglycan. *Mol. Cell* **4**, 633-639.
Tickle, C. and Munsterberg, A. (2001). Vertebrate limb development–the early stages in chick and mouse. *Curr. Opin. Genet. Dev.* **11**, 476-481.
van Eeden, F. J., Granato, M., Schach, U., Brand, M., Furutani-Seiki, M., Haffter, P., Hammerschmidt, M., Heisenberg, C. P., Jiang, Y. J., Kane, D. A. et al. (1996). Genetic analysis of fin formation in the zebrafish, Danio rerio. *Development* **123**, 255-262.
Westerfield, M. (1995). The zebrafish book. A guide for the laboratory use of zebrafish (Danio rerio). 4th edn., Eugene, Oregon: University of Oregon Press.
Xu, X. L., Weinstein, M., Li, C. L. and Deng, C. X. (1999). Fibroblast growth factor receptors (FGFRs) and their roles in limb. *Cell Tissue Res.* **296**, 33-43.
Zak, B. M., Crawford, B. E. and Esko, J. D. (2002). Hereditary multiple exostoses and heparan sulfate polymerization. *Biochim. Biophys. Acta* **1573**, 346-355.
Zwilling, E. (1959). Interaction between ectoderm and mesoderm in duck-chicken limb bud chimaeras. *J. Exp. Zool.* **142**, 521-532.